



Theoretical Studies on Formation Mechanism of Levoglucosan in Pyrolysis of Cellobiose

WEIJUAN LAN¹ and JINBAO HUANG^{2,*}

¹College of Vehicle and Motive Power Engineering, Henan University of Science and Technology, Luoyang 471003, P.R. China

²School of Science, Guizhou Minzu University, Guiyang 550025, P.R. China

*Corresponding author: Tel./Fax: +86 851 3610156; E-mail: huangjinbao76@126.com

Received: 20 July 2013;

Accepted: 14 March 2014;

Published online: 5 July 2014;

AJC-15447

The pyrolysis mechanism of cellobiose as a model compound was investigated using density functional theory methods at B3LYP/6-31++G(d,p) level. Three possible pyrolytic pathways were proposed and the standard thermodynamic and kinetic parameters in each reaction pathway were calculated at different temperatures. In pathway 1, two free radicals **IM**₁ and **IM**₂ are formed through homolytic cleavage of glycosidic bond and the homolysis reaction is endothermic with an energy of 316.65 kJ/mol. **IM**₁ is further converted to levoglucosan **P**₁ via transition state **TS**₁ with an energy barrier of 211.51 kJ/mol. In pathway 2, levoglucosan **P**₁ and glucopyranose **P**₂ are formed through concerted reaction via transition state **TS**₃ with an energy barrier of 270.09 kJ/mol. Compared to reaction pathway 1, the concerted reaction pathway 2 is kinetically favorable and levoglucosan is formed mainly through concerted reaction mechanism. In pathway 3, addition of H⁺ to cellobiose would enhance the breakage of glycosidic bond, but the intermediate **IM**₃ formed can hardly be converted to levoglucosan.

Keywords: Levoglucosan, Formation mechanism, Cellobiose, Pyrolysis, Density functional theory.

INTRODUCTION

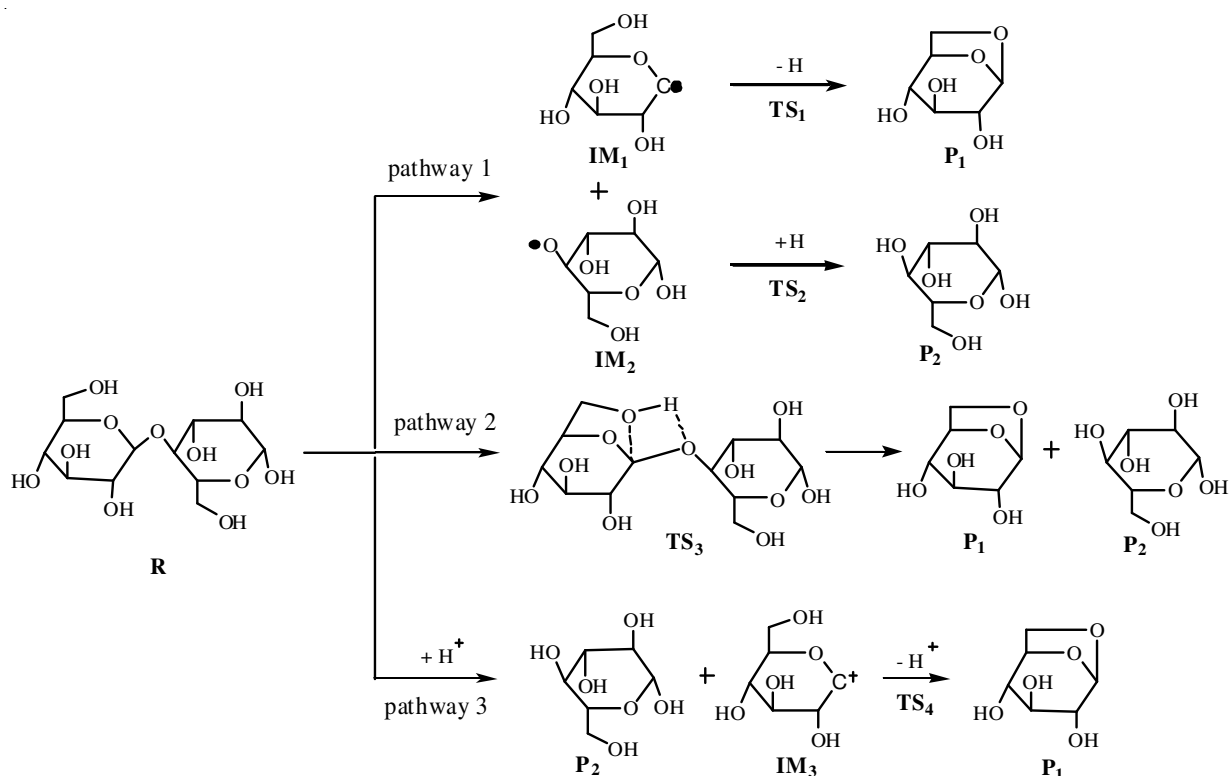
Faced by the increasingly severe problems about energy shortage and environmental pollution around the world, people begin to pay more and more attentions to biomass energy, which is a kind of renewable and clean energy¹⁻⁴. Biomass liquefaction technology that generates bio-oil is considered as the most promising technology among technical routes of utilizing biomass, because bio-oil, as one kind of liquid product, has many advantages, such as convenient storage and transportation as well as high energy density. Cellulose is the most abundant renewable resource in nature and as the major component of biomass, its pyrolytic behavior reflects the whole biomass pyrolysis law by a huge margin. So the study of cellulose pyrolysis mechanism contributes to understanding the performance and the formation mechanism of bio-oil.

For the previous research of cellulose pyrolysis mechanism, most researchers laid emphasis on experimental studies to explore the ratio of tar, gases and coke in different conditions⁵⁻⁷. Also, thermogravimetric analyses were performed to confirm the pyrolysis characteristics of cellulose and kinetic models of cellulose pyrolysis were constructed to attain the kinetic parameters⁸⁻¹⁰. However, there are few researches about formation mechanisms of main products and evolutionary processes of intermediates during cellulose pyrolysis. Because

cellulose pyrolysis is a series of complex reactions and gives inseparable mixtures, it is difficult to analyze detailed mechanism through experiments. So people gradually pay more attentions to employing theoretical methods to study the pyrolysis mechanism and to forecast possible reaction pathways¹¹⁻¹³. The experimental results of cellulose fast pyrolysis^{6,14} showed that levoglucosan was the most important component and its proportion in bio-oil was about 45-85 w. %. In order to understand the formation mechanism of levoglucosan, the pyrolysis processes of cellobiose (a circulation unit of cellulose) as a model compound were investigated and the thermodynamic and dynamic parameters in each reaction pathway at different temperatures were calculated using density functional theory methods at B3LYP/6-31++G(d,p) level in this paper.

DESIGN OF REACTION PATHWAYS

There are different views on the formation mechanism of levoglucosan. Richards¹⁵ reported that the heterolysis of glycosidic bond led to the formation of glucose cation, which could be converted to levoglucosan (1,6-anhydro-β-D-glucopyranose) through transglycosylation reaction. Mamleev *et al.*¹⁶ reported that levoglucosan and glucopyranose could be formed through concerted reaction via a transition state with a four-member ring structure (shown in pathway 2 in **Scheme-I**). In



Scheme-I: Design of reaction pathways of cellobiose pyrolysis

order to explore the formation mechanism of levoglucosan, three kinds of pyrolysis reaction pathways of cellobiose as a model compound are designed according to related documents¹⁵⁻¹⁷ and experiences (**Scheme-I**). In pathway 1, two free radicals **IM₁** and **IM₂** are formed through homolysis of glycosidic bond, then **IM₁** goes through dehydrogenation to form levoglucosan **P₁** via **TS₁** and **IM₂** goes through hydrogenation to form glucopyranose **P₂** via **TS₂**. In pathway 2, **P₁** and **P₂** are formed through concerted reaction via transition state **TS₃**. In pathway 3, glucopyranose and a cation **IM₃** are generated by the addition of a hydron to cellobiose and then the cation **IM₃** is converted to levoglucosan.

Calculations methods

All calculations were completed using Gaussian 03 suites of programs¹⁸. The equilibrium geometries of reactant, intermediates, transition states and products were fully optimized by using B3LYP with the 6-31++G(d,p) basis set. The transition states were located by TS method and were confirmed by visual inspection of the imaginary frequency using Gaussview and by IRC calculations. Activation energies (the reaction energy barriers) for reactions were estimated as the relative energies, including ZPE (zero-point energy correction), between the transition state and the reactant. Reactants, intermediates and products had no imaginary frequencies, whereas transition states had exactly one imaginary frequency. The energies of the optimized reactant and products at different temperatures (298, 400, 550, 680, 800 and 950 K) were calculated by adding TEMPERATURE key word in the frequency calculation route section and the standard thermodynamic changes were energies differences between the reactants and the products, including the ZPE.

RESULTS AND DISCUSSION

Selected parameters of the optimized geometries: The optimized structure parameters of the reactant **R**, intermediates **IM₁-IM₃**, transition states **TS₁-TS₃** and products **P₁** and **P₂** at B3LYP/6-31++G(d,p) level are shown in Table-1. Every atom is marked with a serial number. Based on vibration frequency analysis of reactant, intermediates, transition states and products, a transition state has only one imaginary frequency (**TS₁**: -1429.62, **TS₂**: -895.63, **TS₃**: -231.01) and the reactant, intermediates and products have no imaginary frequency.

Kinetic analysis of pyrolysis processes of each reaction pathway: The total energy values of stationary points (namely the reactant, transition states, intermediate and products), calculated at B3LYP/6-31++G(d,p) level with ZPE correction, were listed in Table-2, by which relative energy values can be obtained, such as the values marked in Fig. 1.

The potential energy profiles along reaction pathways 1 and 2 are shown in Fig. 1. In pathway 1, two free radicals **IM₁**

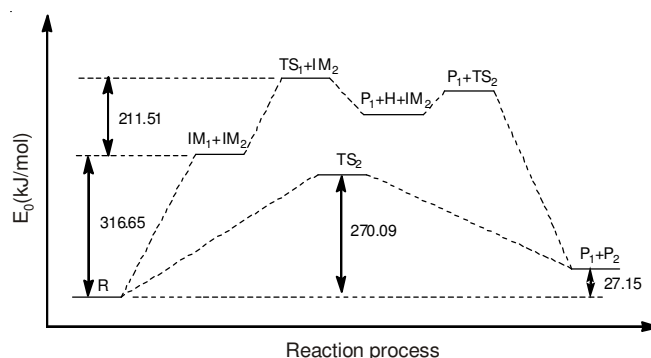


Fig. 1. Potential energy profiles along reaction pathways

TABLE-1
OPTIMIZED STRUCTURE PARAMETERS OF THE REACTANTS, THE INTERMEDIATES, THE PRODUCTS AND THE TRANSITION STATE [BOND LENGTH: (Å); BOND ANGLE/ DIHEDRAL ANGLE: (°)]

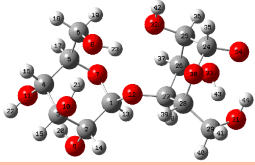

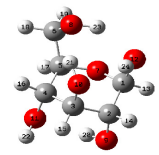

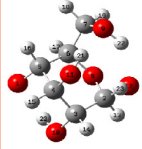

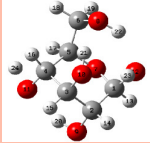
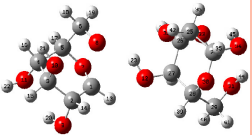
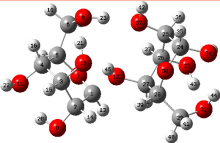
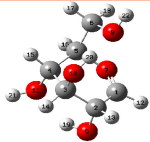
Species	Structural parameters		
	Bond length	Bond angle	Dihedral angle
R 	R(1,2) 1.5405 R(1,7) 1.4090 R(2,3) 1.5446 R(3,4) 1.5459 R(5,7) 1.4428 R(1,12) 1.4316 R(12,27) 1.4290	A(2,1,7) 112.43 A(1,2,3) 112.49 A(2,3,4) 110.11 A(4,5,6) 115.16 A(1,7,5) 121.81 A(7,1,12) 111.67 A(1,12,27) 117.59	D(7,1,2,3) -50.01 D(1,2,3,4) 50.54 D(3,4,5,6) -89.90 D(1,2,3,10) -76.56 D(1,7,5,6) 89.50 D(7,1,12,27) -117.44 D(7,5,6,8) -72.65
P₁ 	R(1,2) 1.5422 R(1,7) 1.4126 R(2,3) 1.5484 R(3,4) 1.5556 R(5,6) 1.5306 R(1,8) 1.4440	A(1,7,5) 102.38 A(1,2,3) 108.65 A(3,4,5) 111.70 A(4,5,6) 113.73 A(7,5,6) 100.11 A(2,1,8) 110.24	D(7,1,2,3) -65.35 D(1,2,3,4) 44.89 D(7,5,6,8) -36.60 D(3,4,5,6) -54.71 D(12,1,2,9) -62.90 D(5,7,1,8) -40.02
P₂ 	R(1,2) 1.5388 R(1,7) 1.4181 R(2,3) 1.5446 R(3,4) 1.5440 R(5,6) 1.5310 R(5,7) 1.4385	A(1,7,5) 120.28 A(1,2,3) 109.23 A(3,4,5) 113.76 A(4,5,6) 114.96 A(7,5,6) 111.69 A(2,1,12) 110.89	D(7,1,2,3) -56.94 D(1,2,3,4) 56.95 D(7,5,6,8) -70.09 D(3,4,5,6) -91.25 D(12,1,2,9) -165.79 D(5,7,1,2) 50.47
IM₁ 	R(1,2) 1.5042 R(1,7) 1.3784 R(2,3) 1.5469 R(3,4) 1.5453 R(5,6) 1.5348 R(5,7) 1.4409	A(1,7,5) 116.70 A(1,2,3) 112.04 A(3,4,5) 113.90 A(4,5,6) 116.74 A(7,5,6) 108.10 A(2,1,7) 118.47	D(7,1,2,3) -46.63 D(1,2,3,4) 45.97 D(7,5,6,8) -59.17 D(3,4,5,6) -77.02 D(12,1,2,9) -60.64 D(9,2,3,10) 155.54
IM₂ 	R(1,5) 1.3561 R(4,5) 1.6043 R(2,3) 1.5364 R(3,4) 1.5478 R(5,6) 1.5564 R(6,8) 1.4356	A(1,5,4) 104.97 A(2,3,4) 110.99 A(3,4,5) 107.06 A(4,5,6) 112.15 A(2,8,6) 120.63 A(5,4,15) 106.99	D(1,5,4,3) 69.68 D(1,5,6,7) 154.47 D(7,6,8,2) 90.64 D(3,4,5,6) -51.69 D(10,3,4,11) 168.53 D(9,7,6,8) -66.63
TS₁ 	R(1,2) 1.5199 R(1,7) 1.3751 R(2,3) 1.5475 R(6,8) 1.4527 R(8,22) 1.3613 R(1,8) 1.8028	A(1,7,5) 105.02 A(1,2,3) 110.65 A(3,4,5) 111.82 A(4,5,6) 115.08 A(5,6,8) 105.52 A(6,5,7) 102.98	D(7,1,2,3) -57.70 D(1,2,3,4) 42.11 D(7,5,6,8) -40.19 D(3,4,5,6) -56.67 D(2,1,7,5) 69.43 D(9,2,3,10) 155.76
TS₂ 	R(1,2) 1.5377 R(1,7) 1.4236 R(2,3) 1.5404 R(3,4) 1.5908 R(4,11) 1.3446 R(11,24) 2.1777	A(1,7,5) 121.11 A(1,2,3) 110.10 A(3,4,5) 110.49 A(4,5,6) 113.65 A(3,4,11) 108.51 A(4,11,24) 111.29	D(7,1,2,3) -57.44 D(1,2,3,4) 59.02 D(7,5,6,8) -67.16 D(3,4,5,6) -91.03 D(10,3,4,11) -166.79 D(5,7,1,2) 50.76
TS₃ 	R(1,2) 1.5048 R(1,7) 1.3611 R(2,3) 1.5394 R(6,8) 1.3536 R(1,8) 2.3588 R(1,12) 2.9232	A(2,1,7) 123.49 A(1,2,3) 115.19 A(2,3,4) 108.15 A(5,6,8) 107.56 A(1,7,5) 113.59 A(7,1,13) 111.90	D(7,1,2,3) -32.88 D(1,2,3,4) 35.04 D(3,4,5,6) -60.45 D(1,2,3,10) -91.68 D(1,7,5,6) 76.68 D(5,7,1,13) -169.25
R+H 	R(1,2) 1.5407 R(1,7) 1.3485 R(2,3) 1.5397 R(5,7) 1.4653 R(1,12) 1.5729 R(12,27) 1.4797	A(2,1,7) 117.13 A(1,2,3) 107.52 A(2,3,4) 109.46 A(1,7,5) 122.62 A(7,1,12) 108.35 A(1,12,27) 123.81	D(7,1,2,3) -51.53 D(1,2,3,4) 58.88 D(3,4,5,6) -94.95 D(1,2,3,10) -62.76 D(1,7,5,6) 104.39 D(7,1,12,27) -119.99
IM₃ 	R(1,2) 1.4929 R(1,7) 1.2688 R(2,3) 1.5397 R(5,7) 1.5002 R(6,8) 1.4226 R(1,12) 1.0899	A(1,7,5) 121.28 A(1,2,3) 116.06 A(3,4,5) 114.49 A(4,5,6) 119.63 A(7,5,6) 105.31 A(2,1,7) 125.19	D(7,1,2,3) -20.25 D(1,2,3,4) 34.41 D(7,5,6,8) -57.56 D(3,4,5,6) -72.92 D(12,1,2,9) -69.22 D(9,2,3,10) 162.38

TABLE-2
ENERGY OF THE REACTANT, INTERMEDIATES, TRANSITION STATES
AND PRODUCTS AT B3LYP/6-31++G(d,p) LEVEL (UNIT: HARTREE)

Species	E	Species	E	Species	E	Species	E
R	-1297.57301	IM ₁	-611.11846	IM ₂	-686.33395	TS ₁	-611.037899
TS ₂	-686.813637	P ₁	-610.57433	P ₂	-686.98833	TS ₃	-1297.47013
R + H ⁺	-1297.91702	IM ₃	-610.89457	H	-0.50032	–	–

and IM₂ are generated through homolysis of glycosidic bond and the reaction is endothermic with an energy of 316.65 kJ/mol. The intermediate IM₁ is further converted to levoglucosan P₁ via transition state TS₁ with an energy barrier of 211.51 kJ/mol and the reaction is a dehydrogenation, which is an endothermic reaction with an energy of 115.01 kJ/mol. The intermediate IM₂ may go through hydrogenation to form glucopyranose P₂ via TS₂ with a low energy barrier of 54.16 kJ/mol and the reaction is an exothermic reaction with an energy of 404.51 kJ/mol. In pathway 2, P₁ and P₂ are formed through concerted reaction via TS₃ with an energy barrier of 270.09 kJ/mol. It is clear from the potential energy profiles in Fig. 1 that the potential barrier of the concerted reaction, pathway 2, is lower than the total potential barrier of the step-by-step reaction, pathway 1, which indicates that reaction pathway 2 is kinetically favorable in pyrolysis of cellobiose and levoglucosan P₁ is formed mainly through concerted reaction mechanism.

Effect of hydrion on pyrolysis: The experimental results of cellulose pyrolysis under the acid pretreatment^{19,20} showed that the degree of polymerization of cellulose in the case of acid pretreatment decreased significantly and the yield of levoglucosan decreased dramatically, but the yield of the small molecule products (such as CHOCH₂OH, CH₂O, CO) increased. The results indicates that hydrion (H⁺) has significant effect on cellulose pyrolysis. In order to comprehend the effect of hydrion on pyrolysis of cellulose, pathway 3 is proposed in pyrolysis of cellobiose added hydrion. The calculation results show that the structure of cellobiose added hydrion changes obviously. It can be seen from the structure of R + H⁺ in Table-1 that the glycosidic bond C(1)-O(12) has been lengthened obviously from R(1,12) = 1.4316 Å in R to R(1,12) = 1.5729 Å in R + H⁺ and hemiacetal linkage C(1)-O(7) has also been shortened from R(1,7) = 1.4090 Å in R to R(1,7) = 1.3485 Å in R + H⁺. In pathway 3, a cation IM₃ and P₂ are formed through breakage of glycosidic bond C(1)-O(12) and the reaction is endothermic with a low energy of 89.59 kJ/mol. In the process of conversion of IM₃ to P₁ + H⁺, neither any transition state nor the stable configuration of P₁ + H⁺ can be attained by optimizing repeatedly, which indicates that it is difficult for the intermediate IM₃ to be converted to levoglucosan. It can be seen from the optimized structure of IM₃ shown in Table-1 that the hemiacetal linkage C(1)-O(7) in IM₃ (1.2688 Å) is close to double bond and it is easier for IM₃ to go through a ring-opening reaction to form small molecule products, such as CHOCH₂OH, CH₂O, CO. The above analysis shows that addition of H⁺ to cellobiose would enhance the breakage of glycosidic bond, but the intermediate IM₃ formed can hardly be further converted to levoglucosan, which results in decrease in the yield of levoglucosan. The above analysis is accordant to related experimental results^{19,20}.

Thermodynamic analysis of pyrolysis process: The thermodynamic parameters, in cellobiose pyrolysis generating levoglucosan and glucopyranose at different temperatures (298, 400, 550, 680, 800, 950 K) at B3LYP/6-31++G(d,p) level are shown in Fig. 2. It is can be seen from Fig. 2 that of pyrolysis reaction shows limited temperature-dependency and values are all positive, indicating an endothermic nature of pyrolysis process., an important parameter in thermodynamic analysis, can be used to judge the spontaneity of a reaction and the percent conversion of products. It is clear from Fig. 2 that values are highly temperature-dependent. At 298 K, of cellobiose pyrolysis are positive, which indicates pyrolysis reaction can not occur spontaneously. However, with the increase of temperature, of pyrolysis reaction becomes negative above 400 K, which indicates pyrolysis reaction can occur spontaneously above 400 K.

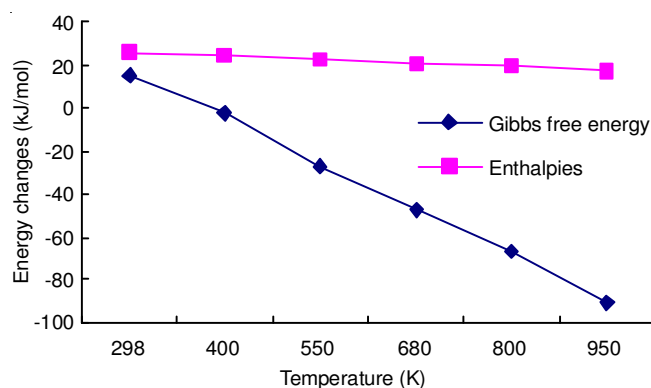


Fig. 2. Relationship between enthalpy and Gibbs free energy changes and temperature

Conclusion

In this work, three possible pyrolytic pathways of cellobiose as a model compound were proposed and thermodynamic and kinetic parameters in each reaction pathway were calculated by density functional theory methods at B3LYP/6-31G++(d,p) level. The calculation results show that two free radicals IM₁ and IM₂ are formed by homolysis of glycosidic bond and the reaction is endothermic with an energy of 316.65 kJ/mol. And then IM₁ react further to form levoglucosan P₁ via transition state TS₁ with an energy barrier of 211.51 kJ/mol. In pathway 2, levoglucosan P₁ and glucopyranose P₂ are formed by concerted reaction via TS₃ with an energy barrier of 270.09 kJ/mol. Comparing energy barriers of rate-determining steps in pathways 1 and 2, it is easy to know that the potential barrier of pathway 2 is lower than that of pathway 1, which indicates that reaction pathway 2 is kinetically favorable in pyrolysis of cellobiose and P₁ is formed mainly by concerted reaction mechanism. In pathway 3, a cation IM₃ and P₂ are

generated by breakage of glycosidic bond C(1)-O(12) and the reaction is endothermic with an energy of 89.59 kJ/mol. Addition of H⁺ to cellobiose would enhance the breakage of glycosidic bond, but the intermediate **IM**₃ formed can hardly be further converted to levoglucosan, which results in decrease in the yield of levoglucosan. Thermodynamic analysis shows that cellobiose pyrolysis is endothermic reaction and can occur spontaneously above 400 K.

ACKNOWLEDGEMENTS

This work was supported by the National Natural Science Foundation of China (No. 51266002), the Natural Science Research Funds of the Department of Education of Guizhou Province (No. [2013]405), the Open Research Funds of Key Laboratory of Low-grade Energy Utilization Technologies and Systems (Chongqing University), Ministry of Education of China (No. LLEUTS-201303), the Science and Technology Funds of Guizhou province (No. [2012]2188), Dean University of Science and Technology Talent Introduction Fund Projects (No. 09001759) and Education Department of Henan Province Science and Technology Key Project (No. 14B470020).

REFERENCES

1. D.E. Arseneau, *Can. J. Chem.*, **49**, 632 (1971).
2. J.B. Huang, C. Liu and S.A. Wei, *Acta Chim. Sin.*, **67**, 2081 (2009).
3. M. Statheropoulos and S.A. Kyriakou, *Anal. Chim. Acta*, **409**, 203 (2000).
4. A.V. Bridgwater and G.V.C. Peacocke, *Renew. Sustain. Energy Rev.*, **4**, 1 (2000).
5. M.J. Antal and J.G. Varhegyi, *Ind. Eng. Chem. Res.*, **34**, 703 (1995).
6. Y.F. Liao, Z.Y. Luo, S.R. Wang, C.J. Yu and K.F. Cen, *J. Fuel Chem. Technol.*, **31**, 133 (2003).
7. J. Piskorz, D. Radlein and D.S. Scott, *J. Anal. Appl. Pyrolysis*, **9**, 121 (1986).
8. J.L. Banyasz, S. Li, J.L. Lyons-Hart and K.H. Shafer, *J. Anal. Appl. Pyrolysis*, **57**, 223 (2001).
9. V. Mamleev, S. Bourbigot and J. Yvon, *J. Anal. Appl. Pyrolysis*, **80**, 151 (2007).
10. T. Sonobe and N. Worasuwannarak, *Fuel*, **87**, 414 (2008).
11. H.J. Wang, Y. Zhao, C. Wang, Y. Fu, Q.X. Guo and Q.Z. Shi, *Acta Chim. Sin.*, **67**, 893 (2009).
12. J. Huang, C. Liu, S. Wei, X. Huang and H. Li, *J. Mol. Struct. (Theochem)*, **958**, 64 (2010).
13. C. Liu, J. Huang, X. Huang, H. Li and Z. Zhang, *Comput. Theoretical Chem.*, **964**, 207 (2011).
14. Y.F. Liao, S.R. Wang, Z.Y. Luo, H. Tang, C.J. Yu, J.S. Zhou and K.F. Cen, *J. Zhejiang Univ. Eng. Sci.*, **37**, 82 (2003).
15. G.N. Richards, *J. Anal. Appl. Pyrolysis*, **10**, 251 (1987).
16. V. Mamleev, S. Bourbigot, M. Le Bras and J. Yvon, *J. Anal. Appl. Pyrolysis*, **84**, 1 (2009).
17. S.R. Wang, Y.F. Liao, H. Tan, Z.Y. Luo and K.F. Cen, *J. Fuel Chem. Technol.*, **31**, 317 (2003).
18. M.J. Frisch, G.W. Trucks, H.B. Schlegel, G.E. Scuseria, M.A. Robb, J.R. Cheeseman, J.A. Montgomery Jr., T. Vreven, K.N. Kudin, J.C. Burant, J.M. Millam, S.S. Iyengar, J. Tomasi, V. Barone, B. Mennucci, M. Cossi, G. Scalmani, N. Rega, G.A. Petersson, H. Nakatsuji, M. Hada, M. Ehara, K. Toyota, R. Fukuda, J. Hasegawa, M. Ishida, T. Nakajima, Y. Honda, O. Kitao, H. Nakai, M. Klene, X. Li, J.E. Knox, H.P. Hratchian, J.B. Cross, C. Adamo, J. Jaramillo, R. Gomperts, R.E. Stratmann, O. Yazyev, A.J. Austin, R. Cammi, C. Pomelli, J.W. Ochterski, P.Y. Ayala, K. Morokuma, G.A. Voth, P. Salvador, J.J. Dannenberg, V.G. Zakrzewski, S. Dapprich, A.D. Daniels, M.C. Strain, O. Farkas, D.K. Malick, A.D. Rabuck, K. Raghavachari, J.B. Foresman, J.V. Ortiz, Q. Cui, A.G. Baboul, S. Clifford, J. Cioslowski, B.B. Stefanov, G. Liu, A. Liashenko, P. Piskorz, I. Komaromi, R.L. Martin, D.J. Fox, T. Keith, M.A. Al-Laham, C.Y. Peng, A. Nanayakkara, M. Challacombe, P.M.W. Gill, B. Johnson, W. Chen, M.W. Wong, C. Gonzalez and J.A. Pople, Gaussian 03, Gaussian, Inc., Pittsburgh, PA, (2003).
19. S.R. Wang, Y.F. Liao, Q. Liu, Z.Y. Luo and K.F. Cen, *J. Fuel Chem. Technol.*, **34**, 179 (2006).
20. G. Dobeles, D. Meier, O. Faix, S. Radtke, G. Rossinskaja and G. Telysheva, *J. Anal. Appl. Pyrolysis*, **58-59**, 453 (2001).